Preparation and Properties of Poly(dimethyl siloxane)–Colloidal Silica/Functionalized Colloidal Silica Nanocomposites

Sumi Dinkar,[1] A. Dhanabalan,[1] B. H. S. Thimmappa[2]

[1]*Momentive Performance Materials Program, Global Research, GEITC (GE India Technology Centre), Bangalore, India*
[2]*Department of Chemistry, Manipal Institute of Technology, Manipal University, Manipal 576104, India*

Received 11 October 2011; accepted 10 December 2011
DOI 10.1002/app.36667
Published online in Wiley Online Library (wileyonlinelibrary.com).

ABSTRACT: Aqueous spherical colloidal silica (CS) particles with a diameter of 15 ± 5 nm were modified with three different types of monofunctional silane coupling agents to prepare functionalized colloidal silica (FCS) particles. The effects of the surface chemistry of the FCS were studied as a function of the CS/FCS loading in the poly (dimethyl siloxane) (PDMS) polymer. The prepared PDMS–CS/FCS composites were investigated for their physical properties both in the cured and uncured states. The extent of filler–filler and filler–polymer interactions was found to vary with the type of functionalizing agent used to treat the surface of the CS. The filler–filler interaction appeared to be predominant in the PDMS–CS composites, and improved filler–polymer interaction was indicated in the case of the PDMS–FCS composites. The composites containing CS treated with methyltrimethoxysilane exhibited relatively better optical and mechanical properties compared to the other PDMS–FCS composites. This study highlighted the importance of judiciously choosing functionalizing agents to achieve PDMS–FCS composites with predetermined optical and mechanical properties. © 2012 Wiley Periodicals, Inc. J Appl Polym Sci 000: 000–000, 2012

Key words: composites; mechanical properties; polysiloxanes

INTRODUCTION

The mixing of nanoparticles with polymers to form composites has been practiced for decades.[1] For example, a clay-reinforced resin known as *Bakelite* was introduced in the early twentieth century. Even before this, composites were finding applications in the form of nanoparticle-toughened automobile tires prepared by the blending of carbon black, zinc oxide, and/or magnesium sulfate particles with vulcanized rubber.[2] Nanocomposites became more popular at the end of the last century when Toyota researchers revealed that the addition of mica to nylon led to a fivefold increase in the yield and tensile strength of the material.[3,4] Subsequent developments have further contributed to the surging interest in polymer–nanoparticle composites.[5,6] The increased availability of nanoparticles of precise size and shape, the development of instrumentation to probe small particle size, and the unique properties offered by these nanocomposites has significantly contributed to their development.[7] One of the challenges in the formation of well-dispersed nanocomposites is the aggregation of nanoparticles within the matrix due to interparticle interactions. The interactions of nanoparticles with polymers depend on the dispersion and the surface functionalities attached to nanoparticles. These factors are known to have significant impacts on the resulting bulk properties.

Commercially available colloidal silica (CS) particles have been used to make a wide range of poly (dimethyl siloxane) (PDMS) composites, which find applications in diverse fields.[8–15] CS sols have several advantageous properties, such as their commercially availability in large volumes and various sizes, shapes, and dispersions (aqueous and organic), which help to tailor their surface properties. Other advantages include a better wettability, which is assisted by the solvent dispersion, and as a result of these advantages, CS sols require less intensive possessing, and nanoparticles in dispersions are potentially less hazardous compared to nanofluffy powders (fumed silica). These factors make CS as an attractive replacement for the presently used nanofiller fumed silica.

PDMS composites containing modified CS particles have been studied by different research groups for coating and other applications.[16,17] However, there is very limited literature available with regard to their usage as reinforcing fillers in the PDMS matrix. Hence, a key question arises as to whether good reinforcement can be achieved with unstructured

Correspondence to: S. Dinkar (sumi.suvarna@ge.com).

TABLE I
Sample Name and Characterization Results of CS and FCS

Sample name	Type of silane (g)	Thermal degradation with TGA			Carbon and hydrogen content			
					Theoretical[a]		Experimental	
		Total weight loss (0–1000°C)	Weight loss % at 0–200°C	Weight loss % at 200–600°C	(% C)	(% H)	(% C)	(% H)
CS		4.181	2.701	1.113			0.03	0.273
FCS1	PTMS (5.1) + HMDZ (14)	5.072	1.09	2.863	1.852	0.129	2.54	0.6
FCS2	DTES (7.9) + HMDZ (14)	6.201	1.173	4.477	3.448	0.6	2.78	0.79
FCS3	MTMS (3.5) + HMDZ (14)	3.3	1.127	1.627	0.308	0.077	1.03	0.53

[a] We assumed a tridental anchoring of silane.

particles such as CS. Earlier, Castaing[18] reported the formation of a reinforced PDMS elastomer with exceptionally good properties when CS was adsorbed onto PDMS. Most recently, Kwan et al.[19] studied the modification of aqueous CS and their reinforcing capability in PDMS with a two-step process. These studies were based on modified CS with trifunctional functionalizing agents, such as trimethyl and vinyl dimethyl functional silanes. To our surprise, there is very limited literature available related to the CS treated with monofunctional functionalizing agents. Hence, a detailed investigation of the interaction effects involving the nature of functionalizing agents and the loading of functionalized colloidal silica (FCS) in PDMS-based composites is important because of the potential application of such composites in different fields.

In this study, CS was double functionalized with different trialkoxysilanes, including methyltrimethoxysilane (MTMS), phenyltrimethoxysilane (PTMS), and dodecyltrimethoxysilanes (DTES); this was followed by treatment with hexamethyldisilazane (HMDZ) with the molar ratio of CS, trialkoxysilane, and HMDZ kept constant. Various PDMS–FCS composites were prepared by the dispersion of the modified CS in the PDMS matrix; they were cured in the form of sheets and characterized for their mechanical (tensile properties and Shore A hardness) and optical [transmittance (%*T*)] properties. The dispersion of CS particles in the PDMS composites was inferred through transmission electron microscopy (TEM) analyses, and the surface functionalization was inferred by elemental analysis.

EXPERIMENTAL

Materials

Aqueous dispersions (pH 2–4) of CS (viscosity < 3 mPa at 25°C) particles (10–20 nm) were received as samples from Nissan Chemicals (Houston, TX). MTMS, PTMS, HMDZ, and dodecyltrimethoxysilane were procured from Gelest. Triethylamine, isopropyl alcohol, xylene, and 1-methoxy-2-propanol were procured from Aldrich and were used as received. Vinyl-end-capped PDMS with an average molecular weight of about 65,000, hydride functionalized PDMS with an average molecular weight of about 2800, and chloroplatinic acid ethynylcyclohexanol were received from Momentive Performance Materials, Inc., and were used without further purification.

Procedure for the functionalization of CS (to FCS)

A three-necked, round-bottom flask fitted with a reflux condenser and an overhead stirrer was charged with CS dispersion (100 g, 31.14% solid dispersed in water), 1-methoxy-2-propanol (100 g), and monofunctional silane (7.9 g). The resulting mixture was stirred at 80°C for 1 h. Triethylamine (0.5 g) was added to this mixture, and stirring was continued for another 1 h. Subsequently, water was exchanged with 1-methoxy-2-propanol by distillation. The resulting suspension was heated to 60°C, and hexadimethyl disilazane (14.7 g) was added dropwise. The reaction was continued at the same temperature for 2 h to functionalize the unreacted hydroxyls. To this mixture, xylene (150 g) was added slowly with stirring, and 1-methoxy-2-propanol (100 g) was distilled to get the FCS dispersion in xylene. Details of the functionalizing agent are given in Table I.

Procedure for making the PDMS–FCS composites

The cured PDMS–FCS composites were prepared with a two-step process. The first step involved the preparation of the composite base, whereas the second step included the curing of the composite base with the addition of a crosslinker, an inhibitor, and a catalyst. The composite base was prepared by the mixture of PDMS fluid (60 wt %) in a double planetary mixer (DPM) kettle (Ross DPM instrument, Wuxi, China) with FCS (40 wt % FCS dispersed in xylene) at room temperature for a period of 45 min. The FCS dispersion was added in portions (100 mL every 10 min) to ensure homogeneous mixing. Subsequently, the contents were heated to a temperature

TABLE II
Sample Codes and Loading Details Used in the PDMS–CS and PDMS-FCS Composites

Sample name	PDMS loading (wt %)	CS loading (SiO_2)
PDMS–CS10	90	10
PDMS–CS20	80	20
PDMS–CS30	70	30
PDMS–CS40	60	40
PDMS–FCS1-10	90	10
PDMS–FCS1-20	80	20
PDMS–FCS1-30	70	30
PDMS–FCS1-40	60	40
PDMS–FCS2-10	90	10
PDMS–FCS2-20	80	20
PDMS–FCS2-30	70	30
PDMS–FCS2-40	60	40
PDMS–FCS3-10	90	10
PDMS–FCS3-20	80	20
PDMS–FCS3-30	70	30
PDMS–FCS3-40	60	40

of 80°C with concomitant application of a vacuum to remove the volatile dispersion medium for 1 h. The temperature of the kettle was further raised to 110°C and kept at this temperature for 60 min *in vacuo* (10 mbar) to remove any traces of volatiles.

In second step, the composite base was mixed with the required amounts of hydride-functionalized PDMS, ethynylcyclohexanol, and chloroplatinic acid catalyst in a kitchen blender. It was essential to remove air bubbles from the mass with the application of a vacuum before it was cured in a compression-molding machine. The curing of the composite into sheets in the compression-molding machine was done at 170°C with 90 kN of pressure for a period of 10 min. PDMS composites consisting of various loadings (30, 20, and 10 wt %) of FCS were also prepared by a similar procedure (Table II). For the purposes of comparison, uncured/cured PDMS–CS composites were also prepared.

Characterization of the PDMS–FCS composites

The thermal characteristics of the uncured PDMS–CS/FCS composite base was inferred by thermogravimetric analysis (TGA) with a TGA 2950 instrument from TA Instruments waters LLC, DE. We took the TGA measurements by heating a sample kept in a platinum pan from 25 to 700°C at a heating rate of 10°C/min under a nitrogen atmosphere. The rheological properties of the uncured PDMS base composites were inferred with an ARES II strain-controlled rheometer from Rheometric Scientific in the dynamic frequency mode waters LLC, DE. In the rheological measurement, the uncured sample was loaded between two disks (diameter = 25 mm) separated by a distance of 1.5 mm, and the experiments were conducted from an initial frequency of 0.1 rad/s to a final frequency of 100 rad/s with a dynamic strain of 2% and at a constant temperature of 24°C.

The dispersions of CS and FCS within the cured PDMS composite were inferred through TEM analyses. The sample preparation for TEM analysis involved the cutting and blocking of part of the cured sheets. The blocked sample was then faced and microtomed to 100-nm sections with a Leica Ultracut microtome. The functionalization was inferred with Fourier transform infrared (FTIR) spectroscopy analysis (Perkin Elmer Spectrum-GX, USA). The optical properties of the cured PDMS composites ($\sim$ 2 mm thick) were measured with a BYK Gardner spectrometer in the transmission mode (Geretsried, Germany). The static mechanical properties [tensile properties and percentage elongation (%E)] were measured with an Instron instrument (Grove city, PA, USA) according to the protocols specified in ASTM DIN 53504 S2. The elemental analysis (% C and % H) was determined by a combustion analyzer with a Thermo Fischer Scientific instrument (Mumbai, India).

RESULTS AND DISCUSSION

Surface characterization of FCS

The functionalization of the commercial CS (particle size = 15 $\pm$ 5 nm) was inferred from FTIR spectroscopy, elemental analysis (% C and % H), and TGA. The FTIR spectral characteristics of the both commercial CS and FCS are shown in Figure 1. The weak vibration absorption peaks observed at about 2992 cm^{-1} for all of the FCS were attributed to the symmetric and asymmetric stretching of the C—H bond of the organic groups of the functionalizing agents. The weak vibration absorption peaks observed at about 1430 and 700 cm^{-1} in FCS1 were attributed to the bending symmetric and asymmetric vibrations of Si—Ar; this confirmed the phenyl functionality on the silica surface. The absorptions between 950 to 1100 cm^{-1} and at about 785 cm^{-1} were assigned to Si—O—Si stretching (both symmetric and asymmetric) and bending vibrations, respectively. The broad peak at 3000–3800 cm^{-1} was assigned to the —OH stretching vibrations of Si—OH and H_2O. The low-intensity peak at about 950 cm^{-1} was due to the bending vibrations associated with the Si—OH group. Compared to those in commercial CS, the vibration absorption peaks in the region 1000–1300 cm^{-1} were found to be relatively broader for FCS; this indicated the formation of Si—O—Si linkages through the condensation reaction of the surface Si—OH of CS and the Si—OH of hydrolyzed functionalizing agents. The lowering of the area under the curve in the region of 3000–3600 cm^{-1} was considered to indicate the reaction of Si—OH

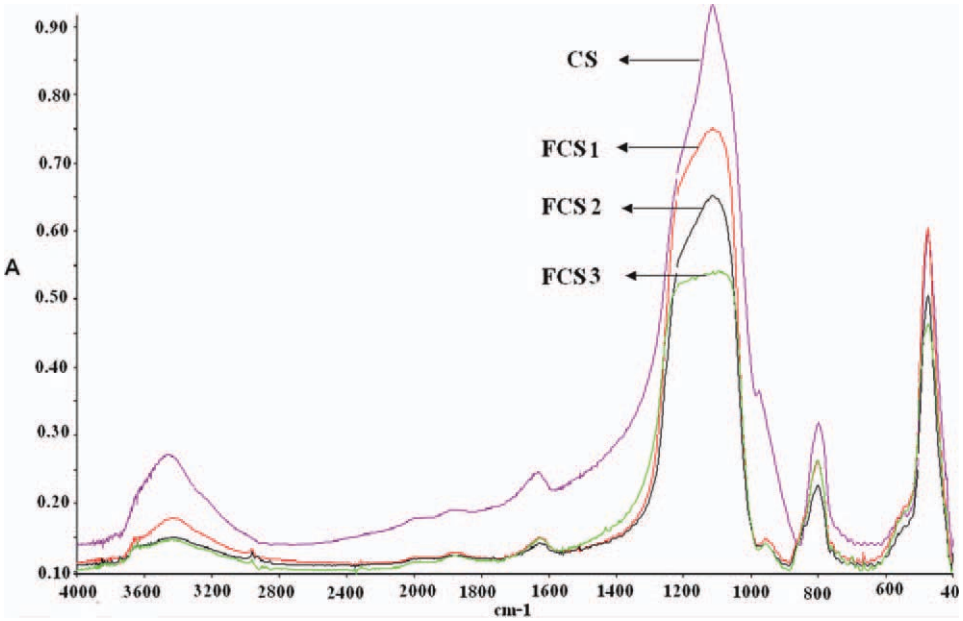

Figure 1 FTIR spectra of commercial CS and FCS (A = absorbance). [Color figure can be viewed in the online issue, which is available at wileyonlinelibrary.com.]

present at the surface of CS with the respective functionalizing agents. The extent of functionalization seemed to vary with the type of organic group of the functionalizing agent.

Further silane coverage of the CS surfaces was determined with TGA and elementary analysis. The TGA results indicate that the unreacted silica showed a weight loss of about 2% before 200°C; this was related to the elimination of physically absorbed water on the surface. The second weight loss (200–600°C) was assigned to the chemically bound water in untreated silica. On the other hand, the treated silica showed a significantly higher weight loss between 200 and 600°C; this was attributed to the debonding of grafted silane functionalizing agents. This confirmed the surface functionalization of CS with silane. Similarly, elemental analysis indicated significantly higher carbon and hydrogen contents with FCS samples and confirmed the surface functionalization of CS with silane. Even though the percentage weight loss (200–600°C) from the TGA results was consistent with carbon and hydrogen results obtained from elemental analysis, there was a difference in the theoretically calculated percentage of carbon versus the experimentally observed results. The observed difference in carbon content weight loss in TGA with the theoretically calculated carbon content was attributed to the reactivity difference of trialkoxysilane with the surface of CS. This could be explained with a simplified mechanistic scheme. The reaction of the surface silanols with the functional groups of trialkoxysilane was expected to yield three types of anchoring onto the silica particles. These monodentate, didentate, and tridentate structures (see Fig. 2) could result from the reaction of one, two, or three alkoxy groups with the silanols on the silica surface. The condensation of trimethylsilanol of the second functionalizing agent (HMDZ) depended on the steric effect of the anchoring group on the surface of silica/hydroxide of the first functionalizing agent.

The morphological characteristics of CS before and after functionalization with different silanes are shown in Figure 3. The TEM image of the commercial CS was indicative of the presence of discrete spherical particles with average particle sizes of 15 ± 5 nm. As seen from the images, the functionalization of CS with different silanes did not influence the morphology of CS significantly; this indicated

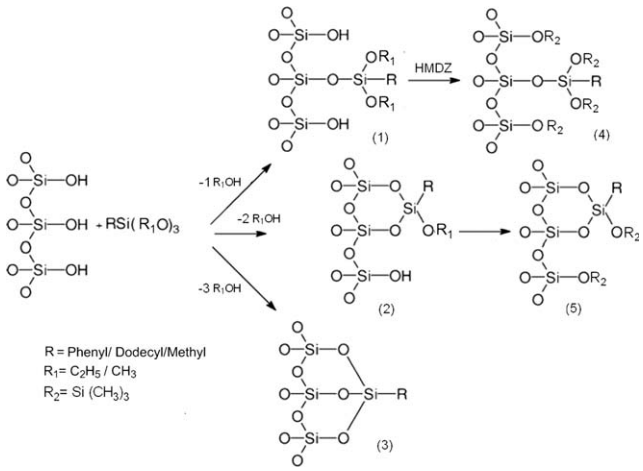

Figure 2 Possible reactions of trialkoxysilanes with CS surface.

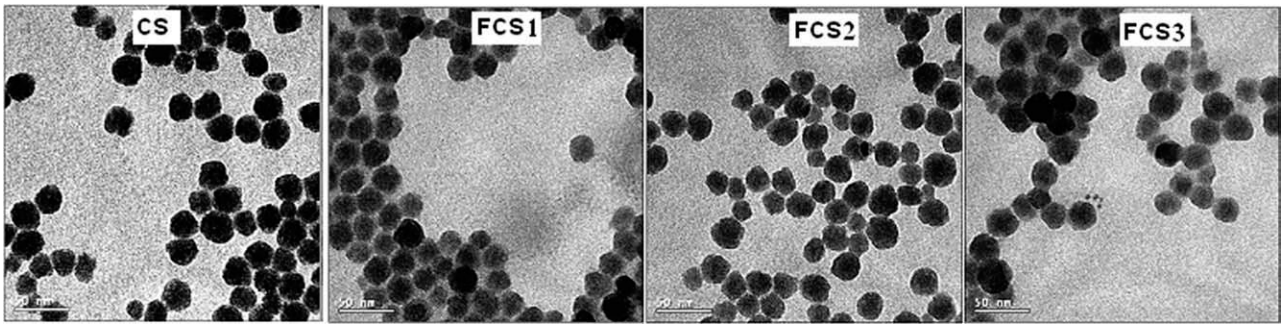

Figure 3 TEM micrographs of the commercial CS and FCS (FCS1, FCS2, and FCS3).

particles are having hydrophobic surface characteristics. All three functionalizing agents seemed to react with silanols and result in complete surface coverage; this, thereby, created repulsion between each them, which led to a discrete particle morphology.

Characterization of the uncured PDMS composites

Thermal characteristics

TGA thermograms of the uncured PDMS–CS/FCS composites at a fixed loading of 40 wt % CS/FCS are depicted in Figure 4. Both the onset degradation temperature and the char residue at elevated temperatures (>650°C) were found to be higher for CS/FCS-containing PDMS composites, and such a trend was similar to that reported for poly(methyl methacrylate)-based hybrid materials containing CS.[20] The thermal degradation of pure PDMS in an inert atmosphere is usually accompanied by depolymerization over the temperature range 400–650°C to produce cyclic oligomers.[21,22] The improvement in the thermal stability of the PDMS–CS/FCS composites as compared to that of the pure PDMS was attributed to the presence of silica, which induced a protective barrier against the thermal degradation of PDMS. The residual weight loss at 700°C for all composites remained at about 40%; this indicated the incorporation of 40 wt % CS/FCS in the PDMS matrix.

Rheological characteristics

Figure 5 represents the changes in the viscosities of the uncured PDMS–CS composites with various loading of CS/FCS dispersed in the PDMS matrix. For the unmodified CS at all loadings and FCS at 10 wt % loading, the viscosity was independent of frequency, as expected of a Newtonian fluid. However, the modified CS viscosity was dependent on the frequency; this was more accentuated as the FCS concentration was increased. The increase in viscosity was in the order PDMS–FCS2 > PDMS–FCS3 > PDMS–FCS1 > PDMS–CS, and the magnitude of increase was found to vary with the type of functionalizing agent, especially at higher loadings of FCS (30–40 wt %). The significantly higher viscosity of FCS2 as compared to FCS1 and FCS3 at all loading levels could be attributed to the structuring of long-chain alkyl chains through self-aggregation of long alkyl chains. This led to higher hydrophobic

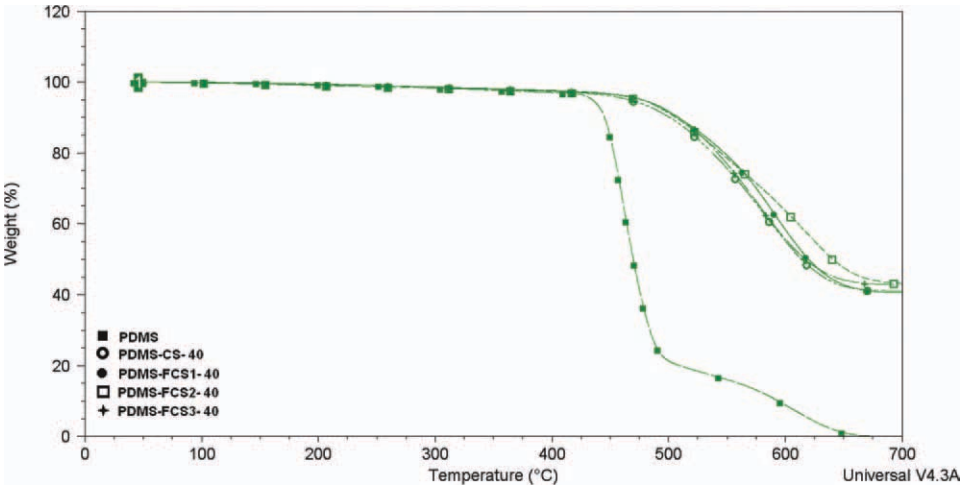

Figure 4 TGA curves of the uncured PDMS–CS composites containing CS40, FCS1-40, FCS2-40, and FCS3-40. [Color figure can be viewed in the online issue, which is available at wileyonlinelibrary.com.]

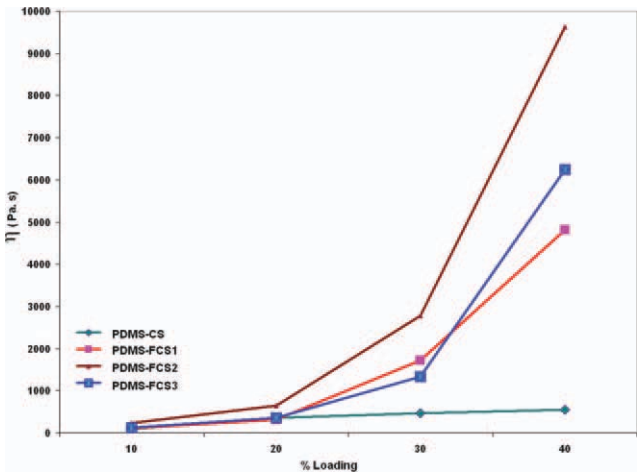

Figure 5 Rheology data of the uncured PDMS composites containing CS, FCS1, FCS2, and FCS3 (η = viscosity). [Color figure can be viewed in the online issue, which is available at wileyonlinelibrary.com.]

surface characteristics[23] and their poor miscibility/compatibility with the polar backbone of the PDMS matrix. The addition of fillers into an elastomer matrix usually results in an increase in the viscosity of the composite, and in general, it is related to the structuring of the filler within the matrix.[24] The observed trend in the variation of increase in the viscosities of the uncured PDMS composites was attributed to the variation of the filler–filler and filler–PDMS interactions derived from different functionalizing agents on the CS surface, which led to different extents of dispersions in PDMS.

Characterization of the cured PDMS–CS/FCS composites

Microscopic analyses

To understand the dispersion of FCS in the cured PDMS composites, PDMS composites containing 40 wt % of differently surfaced FCS particles were analyzed by TEM (Fig. 6). The TEM image of the PDMS composites containing 40 wt % of unfunctionalized CS showed agglomerated particles within the PDMS matrix. However, a uniform dispersion was evident in the case of the PDMS–FCS composites. The formation of larger aggregates in the case of the PDMS–CS composites could be rationalized to stronger filler–filler interactions and weaker filler–matrix interactions formed by hydrogen bonding. The observed uniform dispersion of FCS in PDMS was attributed to the relatively stronger filler–matrix interaction derived from the wetting of particles by the surface structure and their miscibility with the PDMS matrix. The relatively better dispersion observed for the PDMS–FCS3 composite indicated that the methyl functionality on CS particles had a higher degree of miscibility with the PDMS matrix as compared to the phenyl and dodecyl functionalities. The lower dispersion in case of the PDMS–FCS2 composite was due to the higher hydrophobic nature of the dodecyl functionality and a lower wetting capability with the PDMS matrix. Although FCS1 showed a relatively better dispersion than FCS2, the phenyl functionality on the surface of CS seemed to hinder the secondary reaction with HMDZ, or it had lower miscibility with PDMS. A similar trend was observed by Suzuki et al.[23] with fumed silica styrene butadiene rubber (SBR) elastomers. Also, it is well known that the introduction of functionalizing agents by surface treatment decreases the silanols, which reduces the probability of the formation of secondary structures resulting in better dispersions. However, it is not obvious that all types of functionalities show the same degree of dispersion in a given matrix. Our results indicate the importance of choice of functionalizing agents to ensure the uniform dispersion of CS within the PDMS matrix.

Optical characteristics

The optical properties of the PDMS–CS/FCS composites were inferred through %*T* measurements, as shown in Figure 7. The incorporation of CS/FCS particles was found to reduce %*T* of PDMS at all loading levels. This was attributed to the increased scattering of light by fillers (CS/FCS) dispersed within the otherwise transparent PDMS matrix. The

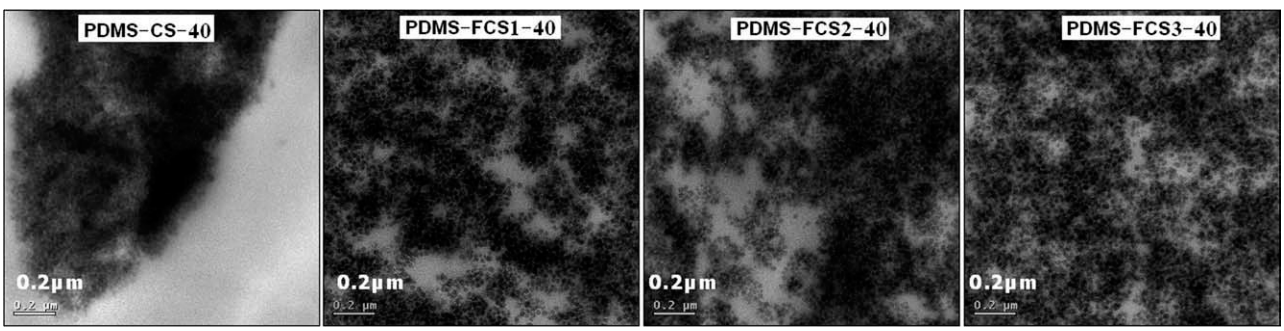

Figure 6 TEM micrographs of the cured PDMS–CS and PDMS–FCS composites containing (a) CS40, (b) FCS1-40, (c) FCS2-40, and (d) FCS3-40.

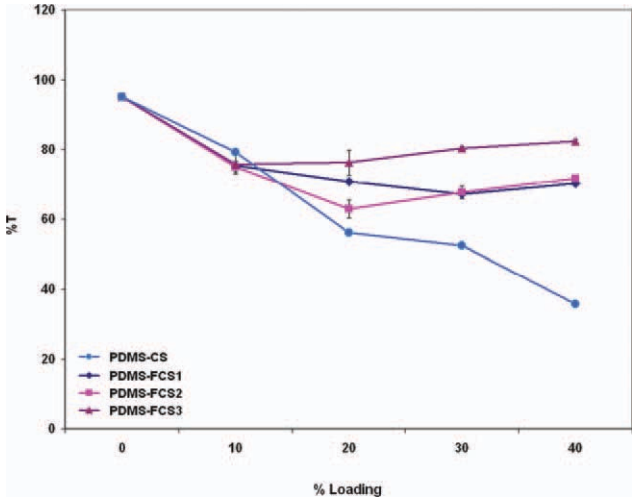

Figure 7 Optical properties of the cured PDMS composites of CS, FCS1, FCS2, and FCS3. [Color figure can be viewed in the online issue, which is available at wileyonlinelibrary.com.]

observed lowering of %*T* was significant with the PDMS–CS composites compared to the PDMS–FCS composites. Among the different PDMS–FCS composites, the PDMS–FCS3 composites showed relatively better %*T* compared to the other two PDMS–FCS composites. Also, an improved %*T* was observed with increased loadings of FCS3; this indicated uniform dispersion across the matrix and space-filling particle structures assisted by surface methyl groups. This was in agreement with the TEM data discussed earlier and indicated a good dispersion of FCS3 within the PDMS matrix with relatively less agglomeration.

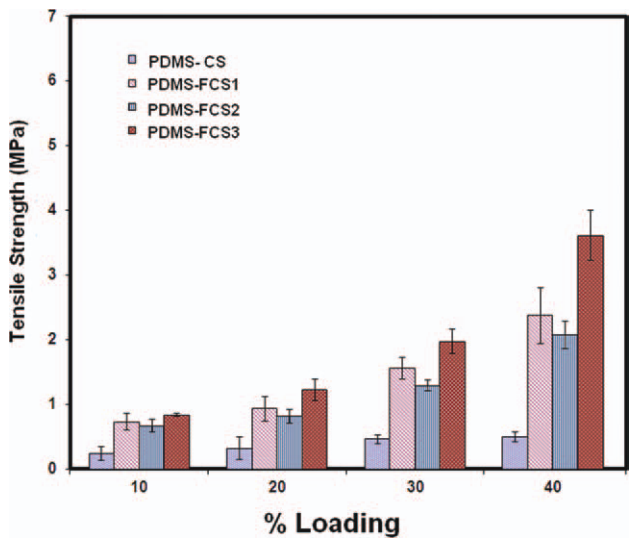

Figure 8 Tensile strength of the cured PDMS composites with different loadings of CS/FCS. [Color figure can be viewed in the online issue, which is available at wileyonlinelibrary.com.]

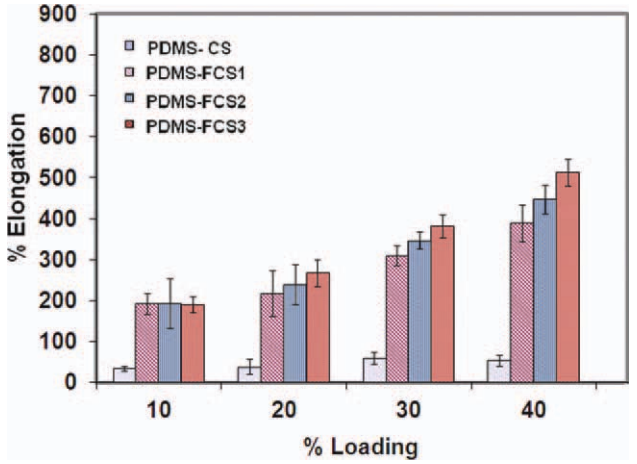

Figure 9 Graph showing the variation of %*E* versus percentage loading of different nanocomposites. [Color figure can be viewed in the online issue, which is available at wileyonlinelibrary.com.]

Mechanical properties

The mechanical properties, namely, the tensile properties and %*E* of the cured PDMS composites containing different loadings of CS/FCS are summarized in Figures 8 and 9. Improved tensile strength and %*E* values were evident for the FCS-filled PDMS composites compared to those of the PDMS–CS composites. Increased tensile strength and %*E* values were observed with increased loading of FCS. The tensile strength observed for the PDMS–FCS composites were in the order FCS3 > FCS1 > FCS2. The difference in the observed variation in the tensile strength results indicated surface-induced filler–filler and filler–polymer interactions and their effect on the overall reinforcing capability. As evidenced from TEM, rheology, and optical studies, FCS3 showed better wetting and space-filling structural characteristics by optimal filler–filler and filler–polymer interactions. The relatively lower tensile strength of FCS2 further confirmed the relatively lesser polymer–filler interactions due to the aggregation of alkyl chains and their incompatibility with the PDMS matrix. On the other hand, FCS1, due to the phenyl functionality, showed a lesser compatibility with the PDMS matrix (methyl backbone) and had lower space-filling characteristics because of the π–π repulsions; this resulted in lower tensile values. Unlike the tensile strength, the elongation at break results followed a different order, which indicated different types of interfacial interactions. The order of increment of %*E* was FCS3 > FCS2 > FCS1. The additions of fillers are known to create chain inhomogeneities that result in increased strain values. Also, when a filler network is strained, the fillers are known to move away as a result chain breaks at different strain levels, as evidenced by the different

values of %*E* in our results. The higher values of %*E* in the case of FCS3 were attributed to the stress transfer of filler particles, whereas the relatively lower %*E* with the FCS1 and FCS2 PDMS composites were due to dewetting and molecular slippage mechanisms, respectively.

CONCLUSIONS

PDMS composites with different loadings of CS and FCS were prepared and characterized both in the cured and uncured states. The uncured composites were used for the thermal and rheological property determination, and the cured composites were analyzed for their compositional, microscopic, optical, and mechanical properties. The extent of filler–filler/filler–polymer interactions was found to vary with the type of functionalizing agent used to treat the surface of CS. In the case of the PDMS–CS composites, filler–filler interactions predominated; this led to inferior mechanical and optical properties. In comparison, the PDMS–FCS composites possessed improved mechanical properties because of improved filler–polymer interactions; this resulted in the uniform dispersion of FCS within the PDMS matrix. The composites containing CS treated with MTMS exhibited relatively better optical and mechanical properties among the different PDMS–FCS composites studied. This study underlined the importance of choosing appropriate functionalizing agents and their interaction with PDMS to obtain PDMS–FCS composites with desired optical and mechanical properties.

The authors thank Chandra Bajgur, S. S. Swayagith, M. B. Pallavi, Avdhut Maldikar, Mihirkumar Patel, and Vivek Khare for helpful discussions. The authors also thank GEITC (GE India Technology Centre), India, for its support.

References

1. Baekeland, L. H. Sci Am Suppl 1909, 68, 322.
2. Goodyear, C. Dinglers Polytech J 1856, 139, 376.
3. Usuki, A.; Kojima, Y.; Kawasumi, M.; Okada, A.; Fukushima, Y.; Kuraochi, Y.; Kamigaito, O. J Mater Res 1993, 8, 1179.
4. Kojma, Y.; Usuki, A.; Kojima, Y.; Kawasumi, M.; Okada, A.; Kurauchi, T.; Kamigaito, O. J Mater Res 1993, 8, 1185.
5. Rowell, M. W.; Topinka, M. A.; McGehee, M. D.; Prall, H.-J.; Dennler, G.; Sariciftci, N. S.; Hu, L.; Gruner, G. Appl Phys Lett 2006, 88, 233506.
6. Barna, E.; Bommer, B.; Kürsteiner, J.; Vital, A.; Trzebiatowski, O. V.; Koch, W.; Schmid, B.; Graule, T. Compos Appl Sci Manuf 2005, 36, 473.
7. Ajayan, P. M.; Schadler, L. S.; Braun, P. V. Wiley-VCH: Weinheim, 2003.
8. Hunter, R. J. Introduction to Modern Colloid Science. Oxford University Press: New York, 1993.
9. Bourgeat-Lami, E.; Lang, J. J Colloid Interface Sci 1998, 197, 293.
10. Kim, J. W.; Kim, L. U.; Kim, C. K. Biomacromolecules 2007, 8, 215.
11. Corrie, S. R.; Lawrie, G. A.; Trau, M. Langmuir 2006, 22, 2731.
12. Kneuer, C.; Sameti, M.; Bakowsky, U. Bioconjug Chem 2000, 11, 926.
13. Hunter, R. J. Foundation of colloid science, 2nd edn, Oxford University Press: Oxford, 2001.
14. Kneuer, C.; Sameti, M.; Haltner, E. G.; Schiestel, T.; Schirra, H.; Schmidt, H.; Lehr, C. M. J Pharm 2000, 196, 257.
15. Bourgeat-Lami, E.; Lang, J. J Colloid Interface Sci 1998, 210, 281.
16. Schulze Nahrup, J.; Gao, Z. M.; Mark, J. E.; Sakr, A. Int J Pharma 2004, 270, 199.
17. Daniels, M. W.; Sefcik, J.; Francis, L. F.; McCormick, V. J Colloid Interface Sci 1999, 219, 351.
18. Castaing, J. C.; Allain, C.; Auroy, P.; Auvray, L.; Pouchelon, A. Europhys Lett 1996, 36, 153.
19. Kwan, K. S.; Harrington, D. A.; Moore, P. A.; Hahn, J. R., Jr.; Degroot, J. V.; Burns, G. T. Rubber Chem Technol 2001, 74, 630.
20. Sugimoto, H.; Daimatsu, K.; Nakanishi, E.; Ogasawara, Y.; Yasumura, T.; Inomata, K. Polymer 2006, 47, 3754.
21. Clarson, S. J.;Semlyen. J. A. Polymer 1986, 27, 91.
22. Camino, G.; Lomakin, S. M.; Lazzari, M. Polymer 2001, 42, 2395.
23. Suzuki, N.; Yatsuyanagi, F.; Ito, M.; Kaidou, H. J Appl Polym Sci 2002, 86, 1622.
24. Kosinski, L. E.; Caruthers, J. M. J Appl Polym Sci 1986, 32, 3393.